Radiopaque Organic−Inorganic Hybrids Based on Poly(D,L-lactide)

Laura Mazzocchetti, Sergio Sandri, and Mariastella Scandola*

Department of Chemistry "G. Ciamician", University of Bologna, and National Consortium of Materials Science and Technology (INSTM), Via Selmi 2, 40126 Bologna, Italy

Anna Bergia and Giampaolo Zuccheri

Department of Biochemistry "G. Moruzzi", University of Bologna, National Center on nanoStructures and bioSystems at Surfaces (S3) of INFM (Modena), and National Consortium of Materials Science and Technology (INSTM), Via Irnerio 48, 40126 Bologna, Italy

Received September 27, 2006; Revised Manuscript Received November 6, 2006

Hybrid organic−inorganic nanocomposites were prepared starting from α,ω-triethoxysilane-terminated poly(D,L-lactic acid) (PDLLA) to be used as potential radiopaque biocompatible coatings for medical devices. The synthesis of the organic phase precursors of given chain length was achieved via anionic polymerization of D,L-lactide using a bifunctional initiator and subsequent triethoxysilane functionalization of the end groups. PDLLA-based ceramers (ceramic polymers) were then synthesized by the sol−gel process at room temperature (rt) in the presence of different amounts of tetraethoxysilane. The rt-synthesized hybrids were then cured (at 80 or 130 °C), and their thermal and viscoelastic properties were investigated. All obtained hybrids were optically transparent, due to the nanometric dimension of the silica particles, and yielded clearly contrasted radiographic images.

Introduction

In the past decade new hybrid materials composed of covalently interconnected organic and inorganic phases have been extensively studied.[1,2] This class of compounds was earlier named "ceramers" (ceramic polymers) by Wilkes et al.[3] and "ormocers" (organically modified ceramic polymers) by Schmidt et al.,[4] with the aim to stress their dual organic and inorganic nature. These materials have gained increasing attention in recent years, due to the remarkable change of the mechanical,[5] thermal,[6−8] electrical,[9] and magnetic[10] properties obtained by the organic−inorganic combination compared with the plain polymeric and ceramic components. In particular, the nanostructured morphology of the inorganic domains strongly affects the physical behavior of the hybrids, leading to interesting properties such as optical transparency.[11]

Although a large number of metal oxides (i.e., those of titanium, zirconium, aluminum, and cerium) were used in the preparation of ceramers, silica is definitely the most widely investigated inorganic phase.[12] A wide spectrum of polymers, i.e., poly(dimethylsiloxane) (PDMS) used in the first reported ceramer,[3,13−15] poly(tetramethylene oxide) (PTMO),[14,16−19] polycaprolactone (PCL),[20−22] polyoxazoline,[23] poly(ether ketone),[24] poly(ethylene oxide),[25] etc., have been employed as the organic phase constituent of ceramers.

The sol−gel process is a well-established method to produce inorganic glasses from metal alkoxide precursors. This is a two-step procedure which involves first metal−alkoxide bond hydrolysis and then polycondensation of the obtained hydroxyl moieties, leading to a three-dimensional inorganic network. Polymer chains can be covalently incorporated at the molecular level into the sol−gel-produced inorganic network by suitable modification of the polymer chain ends with functional groups bearing themselves metal alkoxide units.[26] The conditions required to carry out the sol−gel process are particularly mild: hydrolysis and condensation reactions proceed at low temperature so that the stability of polymeric species is not affected during the synthesis. This feature makes the sol−gel technique the most convenient route to organic−inorganic hybrids.

By using suitable polymers as the organic phase (i.e., PCL, PDMS, PTMO, and chitosan), organic−inorganic hybrids have been developed as bioactive and biocompatible materials.[27,28] Due to its biocompatibility, biodegradability, nontoxicity of degradation products, and good mechanical properties, together with the possibility of obtaining the lactide monomer from renewable resources,[29−31] polylactide (PLA) can be considered a good candidate for the synthesis of ceramers for biomedical applications. Another attractive feature of this aliphatic polyester is that a polymer with a "tailored" chain length can be produced via ring opening "living" anionic polymerization of the cyclic lactide unit.[32] The availability of oligomers with a defined length is important in ceramer synthesis, since this feature affects the thermal and mechanical properties of the hybrid. Hence, the ability to control the polymer chain length represents a way of tuning properties in the final material.

As mentioned above, modification of polymer chain ends with functional groups bearing metal alkoxide units promotes their covalent incorporation into the inorganic network formed via sol−gel reaction. In the case of PLA the monomer is an α,ω-hydroxy acid. To generate the same functionality at both polymer chain ends, a bifunctional initiator able to propagate growing chains on both active sites of the living anionic polymerization process is required. The obtained α,ω-hydroxyl-terminated polylactide can further react at both chain ends with a linker bearing the metal alkoxide unit and finally enter the sol−gel process together with the inorganic phase precursor.

* To whom correspondence should be addressed. E-mail: mariastella.scandola@unibo.it. Fax: +39 051 2099456. Phone: +39 051 2099577.

10.1021/bm060921n CCC: $37.00
Published on Web 01/05/2007

Recent literature concerning surgical and prosthetic applications of biomaterials indicates increasing interest in easy detection of device position by fluoroscopy or X-ray radiography.[33,34] For improved visibility, polymers can be blended with "markers" which block the transmission of X-rays, such as barium sulfate or zirconium dioxide.[35−37] Alternatively, radiopaque polymer−salt complexes can be produced by the incorporation of a radiopaque heavy metal salt, such as bismuth bromide or uranyl nitrate, into an appropriate polymer ligand via chelation.[38,39] As a result, the device appears as a contrasting image against the background of the fluoroscope or X-ray film. Further approaches deal with the synthesis of intrinsically radiopaque polymers by copolymerization of vinyl monomers (i.e., barium or zinc acrylates)[40] or by grafting iodine-containing molecules onto preformed high molecular weight polymers.[41−44] Unfortunately, all mentioned synthetic routes to radiopaque polymeric materials lead to changes of the bulk properties of the reference polymer and may negatively affect device performance.

This drawback can be overcome if a layer of an intrinsically radiopaque material is coated at the surface of the device, an approach by which the impact on bulk properties is very much reduced. Examples of radiopaque coatings are reported in the literature that, however, require the use of rather complex deposition technologies[45,46] or of high-temperature conditions[47,48] not applicable to polymeric materials. In this context, a smart answer to the increasing demand of easily localizable medical devices could be provided by biocompatible and intrinsically radiopaque hybrid coatings, synthesized by the simple sol−gel technique and applicable to a variety of substrates (metals, polymers, fabrics, etc.).

In the present paper we report the synthesis and characterization of nanostructured and radiopaque ceramers containing PLA as the polymeric component. The synthesis of the organic phase precursors, i.e., of PLA-functionalized oligomers with a given chain length, is also described in detail.

Experimental Section

Materials. Tri(ethylene glycol) (TEG; 99%, Aldrich), NaH (60%, w/w, dispersion in mineral oil, Aldrich), THF (absolute ≥99.5% over molecular sieves, Fluka), 3,6-dimethyl-1,4-dioxane-2,5-dione (D,L-lactide; Aldrich), (3-isocyanatopropyl)triethoxysilane (ICPTES; Fluka), tetraethoxysilane (TEOS; Aldrich), and hydrochloric acid (HCl; 37% concentration, Aldrich) were used without further purification.

Synthesis of α,ω-Hydroxyl-Terminated Poly(D,L-lactic acid) (PDLLA-OH). PDLLA-OH having different average chain lengths (n = 10, 20) was synthesized following the procedure here reported for PDLLA-OH (n = 10).

In a nitrogen-flushed two-necked Pyrex flask equipped with a magnetic stirrer, TEG (0.60 g, 4mmol) was dissolved in dry THF (20 mL); NaH, 60% (w/w) dispersion in mineral oil (0.35 g, 8.8mmol), was added and the mixture heated at 50 °C for 2 h. In a second nitrogen-flushed two-necked Pyrex flask equipped with a magnetic stirrer, D,L-lactide (5.78 g, 40 mmol) was dissolved in dry THF (28 mL), and the clear solution was added to the initiator-containing flask. After 1 h the polymerization was terminated by introduction of a stoichiometric amount (4 mmol) of acetic acid dissolved in diethyl ether (1:9). Solvents were evaporated under reduced pressure, and the residue was dissolved in CH_2Cl_2 (30 mL) and extracted with water (3 × 30 mL). The organic phase was then dried with Na_2SO_4 and evaporated under reduced pressure to give 5.47 g of the final PDLLA-OH (n = 10) in 86% yield.

The yield in the case of the synthesis of PDLLA-OH (n = 20) was 68%.

Synthesis of α,ω-Triethoxysilane-Terminated Poly(D,L-lactic acid) (PDLLA-Si). Two PDLLA-Si samples with different average chain lengths (n = 10, 20) were prepared following the procedure reported here for PDLLA-Si (n = 10).

PDLLA-OH (n = 10) was first dried in an oven at 80 °C under vacuum overnight and then heated at 160 °C in a nitrogen-flushed two-necked Pyrex flask equipped with a magnetic stirrer. ICPTES (2 equiv) was added and the mixture allowed to react for 10 min, after which a vacuum was applied for 15 min, keeping the flask at 160 °C. The nitrogen/vacuum cycles were repeated twice to completely remove the unreacted ICPTES. The product was recovered without further purification, leading to PDLLA-Si (n = 10) in 99% yield.

The yield in the case of the synthesis of PDLLA-Si (n = 20) was 99%.

Sol−Gel Preparation of the Hybrids. PDLLA-Si/TEOS mixtures (75:25, 50:50, and 25:75, w/w) were dissolved in THF (1 mL/g of hybrid precursors) and hydrolyzed with a stoichiometric amount of water with respect to the alkoxide functions. HCl was used as a catalyst in a 5:100 HCl:TEOS molar ratio. A representative synthesis was as follows: A 0.5 g sample of TEOS was added to the PDLLA-Si (n = 10) (0.5 g) solution in THF (1.0 mL) and the resulting combination thoroughly mixed until a homogeneous solution was formed. Then deionized water (0.20 mL) and HCl (8 μL) were added under vigorous stirring at ambient temperature for ca. 10 min. The clear solution was then cast onto a Teflon Petri dish and covered with Parafilm to slow the sol−gel process rate. After 96 h at room temperature, the cross-linked material was recovered and was thermally treated for either 2 h in the oven at 80 °C under vacuum or 2 h in the oven at 130 °C without application of the vacuum.

In this work two series of hybrids were prepared starting either from PDLLA-Si (n = 10) (series A) or from PDLLA-Si (n = 20) (series B), labeled AX-Y and BX-Y, respectively. X represents the percentage of TEOS in the sol−gel feed (25, 50, or 75), and Y indicates the applied thermal treatment as follows: Y = 80V means 2 h at 80 °C under vacuum, Y = 130 means 2 h at 130 °C without vacuum, and Y = 0 means that no thermal curing was applied.

Measurements. ^{1}H NMR spectra were recorded on a Varian Gemini 300 MHz spectrometer using $CDCl_3$ solutions. Chemical shifts are reported in parts per million referred to the $CDCl_3$ signal.

Infrared spectra in KBr pellets or on KBr disks were recorded on a Nicolet 380 FT-IR spectrometer.

Thermogravimetric analysis (TGA) measurements were carried out using a TA-TGA 2950 analyzer. The analyses were performed at 10 °C/min from room temperature to 600 °C under N_2 flow.

Differential scanning calorimetry (DSC) measurements were performed using a TA DSC-Q100 apparatus, equipped with an LNCS (liquid nitrogen cooling system) accessory. The samples (about 5 mg) were placed in open Al pans and subjected to heating runs at 20 °C/min from −100 to +80, +100, or +130 °C. Quench cooling was applied between heating scans. T_g values were taken at half-height of the glass transition heat capacity step.

Dynamic mechanical measurements were carried out from −150 to +130 °C by means of a DMTA MkII (Polymer Laboratories Ltd.), using the dual cantilever geometry at 3 Hz and 3 °C/min heating rate. To analyze the hybrid films (200−300 μm thick) in bending mode, two rectangular aluminum plates were used to sandwich the samples as described elsewhere.[49]

X-ray images of the hybrids were recorded on a mammographic apparatus (Diamond MGX, Instrumentarium Co. Imaging Division) equipped with a radiogenic tube, Varian M113SP. The experimental parameters were 22 keV, 4 mA/s, and 21 cm sample-to-detector distance.

A ceramer sample for AFM analysis was synthesized "in situ" on a flat metal disk by the sol−gel process followed by thermal curing. It was then stored at room temperature in a desiccator under vacuum to prevent humidity adsorption from the environment. AFM characterization was carried out on a Veeco Nanoscope IIIA system equipped with a Multimode head. Tapping-mode images and phase-contrast images of 1 × 1 μm were performed with NCH-type noncontact probes (by

Scheme 1. Synthetic Route for α,ω-Triethoxysilane-Terminated Poly(D,L-lactic acid) (PDLLA-Si)[a]

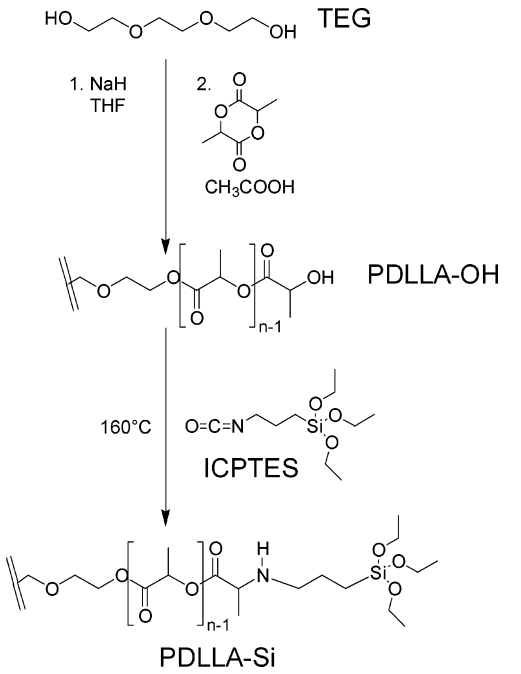

[a] PDLLA-OH and PDLLA-Si are shown as half of the whole macromolecule.

Nanosensors, Wetzlar-Blankenfeld, Germany) operated near their resonance frequency and scanned at approximately 2.7 μm/s linear speed. Phase contrast was optimized by changing the tapping-mode amplitude set point. All images were collected under dry nitrogen flow in an environmental AFM chamber.

Results and Discussion

Synthesis and Characterization of the Diol Oligomeric Precursors PDLLA-OH. Several examples of the use of monoalkoxide initiators for the polymerization of lactide are reported in the literature.[50,51] The polymerization reaction is shown to proceed via acyl−oxygen bond cleavage of the lactide ring: the formed alcoholate is then responsible for chain propagation, and when termination is achieved by addition of acid, a hydroxyl terminal group is created. This is a living polymerization mechanism that allows good control over the molecular weight. In the present case the triethylene glycol disodium salt (NaTEG) initiator is chosen to act as a bifunctional core for the living anionic polymerization of D,L-lactide, thus allowing the synthesis of a telechelic dihydroxy-terminated oligomer of the desired chain length as shown in Scheme 1.

The ^{1}H NMR spectrum of PDLLA-OH ($n = 10$) is reported in the lower part of Figure 1. The spectrum shows the chemical shifts of the poly(D,L-lactide) chains at $\delta = 1.5$ ppm and $\delta = 5.2$ ppm corresponding, respectively, to methyl (d) and methine (c) protons of lactic acid repeating units, as well as the methylene signals of the central TEG unit (a) at $\delta = 3.5-3.7$ ppm. Besides the expected chemical shifts, a broad additional resonance is detected around 4.2−4.4 ppm. The signal is attributed to the overlap of chemical shifts due to protons from the methylene unit connecting the TEG core to the carbonyl carbon of the poly(D,L-lactic) chain (b) and to the methine hydrogen of the terminal lactic group bearing a free hydroxyl moiety (e). Since the b + e signal is not affected by the polymer chain length, it is taken as an internal reference for the evaluation of the polymerization degree (n). By comparison of the b + e signal area with that of the methine hydrogen resonance at $\delta = 5.25$ ppm (c), whose integral depends straightforwardly on the number of repeating lactic acid units in the chain, the polymerization degree is obtained as $n = 3c/(b + e)$. The calculated value ($n = 9.8$) is in good agreement with that obtained from the polymerization feed ($n_{feed} = 10$), in accord with the living character of the anionic polymerization. The same calculation carried out on the ^{1}H NMR spectrum of PDLLA-OH ($n = 20$) satisfactorily agrees with the average degree of polymerization expected from the feed ($n = 19.8$, $n_{feed} = 20$).

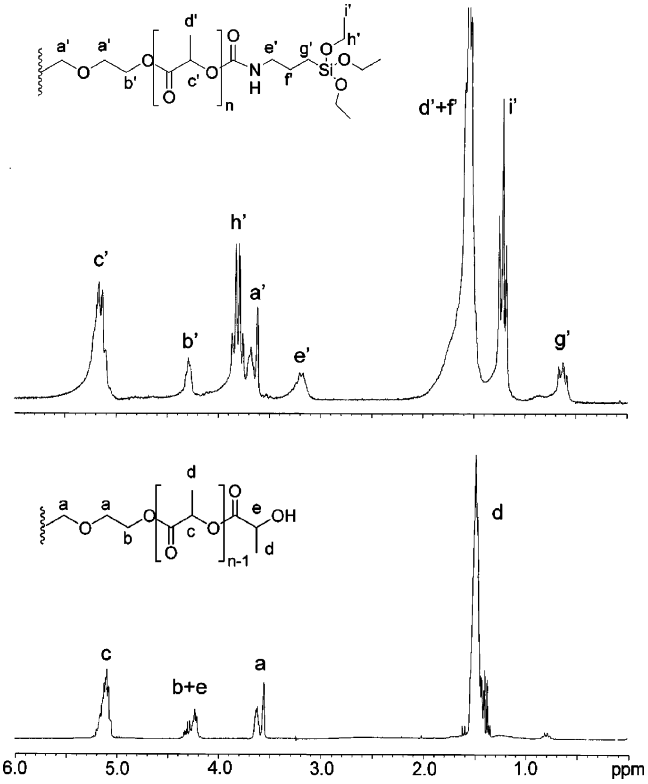

Figure 1. ^{1}H NMR spectra in the 0−6 ppm spectral window of PDLLA-OH (lower spectrum) and PDLLA-Si (upper spectrum) with peak attribution.

Synthesis and Characterization of the Functionalized Oligomeric Precursors (PDLLA-Si). Following the most common literature about functionalization of terminal hydroxyl groups with the isocyanate moiety,[20,21] the reaction was first attempted at 50 °C in THF with 1,4-diazabicyclo[2.2.2]octane (DABCO) as the catalyst and ICPTES in equimolar amount with respect to the hydroxyl terminal units. However, the relatively low molecular weight of the polymers used in this reaction prevented their separation from the catalyst after functionalization by the common solubilization/precipitation method. No alternative route for product purification from the catalyst was found; hence, this synthetic procedure was finally discarded.

With the aim of overcoming the separation drawback, a synthetic pathway avoiding the catalyst was attempted. It is known in the literature that functionalization of terminal hydroxyl moieties of the poly(hydroxy acid) polycaprolactone can be obtained without solvent and catalyst by high-temperature reaction (120−160 °C).[52] The reaction on PDLLA-OH with ICPTES was thus carried out in bulk at 160 °C (Scheme 1), since attempts to work at lower temperature were unsuccessful. A 100% excess of ICPTES was used to force the reaction to completion. Complete removal of unreacted ICPTES was achieved by simple application of a vacuum followed by nitrogen flushing, as confirmed by FT-IR spectroscopy where

Table 1. Thermogravimetric Results of A Series and B Series Hybrids and of Relative Polymeric Precursors

A series		B series	
sample	Δm (rt to 200 °C) (%)	sample	Δm (rt to 200 °C) (%)
PDLLA-Si ($n = 10$)	0.7	PDLLA-Si ($n = 20$)	0.8
A25-0	9.7	B25-0	11.7
A25-80V	3.4	B25-80V	4.8
A25-130	0	B25-130	1.7
A50-0	9.7	B50-0	8.4
A50-80V	4.8	B50-80V	5.4
A50-130	0	B50-130	1.3
A75-0	12.7	B75-0	7.9
A75-80V	3.4	B75-80V	6.7
A75-130	1.5	B75-130	1.5

no signal of the starting isocyanate group was detected at 2270 cm^{-1}. The presence of absorptions at 3380 cm^{-1} from the NH stretching vibration and at 1525 cm^{-1} due to the urethane bond, together with the disappearance of the peak at 3500 cm^{-1} typical of OH stretching, confirms urethane functional group formation.

The actual extent of the functionalization reaction was evaluated by ^1H NMR spectroscopy. As shown in the spectrum of PDLLA-Si ($n = 10$) reported in the upper part of Figure 1, the main chemical shifts related to the poly(D,L-lactic) chain and TEG core discussed above are still present. Due to the reaction with ICPTES, new signals related to ethoxysilane groups (i′ and h′) and to the trimethylene spacer (e′ and g′) appear in the spectrum. The third methylene signal of the aliphatic spacer (f′) overlaps the lactide methyl chemical shift (d′). The chemical shift of the terminal methine proton (e, in the lower spectrum), previously found in the multiplet at $\delta = 4.2-4.4$ ppm, together with the TEG methylene (b), moves downfield in the region of the lactide chain methine hydrogens (c′). The integral ratio of these two modified signals (b′ and c′), when compared with that calculated for the corresponding PDLLA-OH (b + e and c), accounts for a complete conversion of terminal groups. Moreover, there is no evidence of reaction of the ethoxysilane moieties during the functionalization reaction. This observation demonstrates the absence of uncontrolled cross-linking prior to the sol−gel reaction.

It is worth noting that the average degree of polymerization (n) calculated before and after the functionalization reaction does not change, demonstrating the absence of thermal degradation of the polylactide chain in the reaction conditions applied ($T = 160$ °C). It is well-known from the literature that the polylactide chain can easily undergo degradation at high temperature,[53] especially in the presence of water.[54] However, despite the high temperature adopted, careful drying of PDLLA-OH before feeding and the anhydrous reaction environment prevented thermal degradation of the polyester.

To test the thermal stability of the reaction products, both synthesized PDLLA-Si compounds were analyzed by TGA. In both cases, no significant weight loss occurs between room temperature (rt) and 200 °C ($\Delta m < 1\%$, Table 1). Both oligomers have a solid residue at 600 °C (6.3% PDLLA-Si ($n = 10$), 4.9% PDLLA-Si ($n = 20$)) that was tentatively assigned to SiO_2. The experimental amount of residue was compared with the theoretical silica content calculated on the basis of the degree of polymerization of each oligomer, as determined by ^1H NMR. It was found that for PDLLA-Si ($n = 10$) the calculated residue was 5.8%, while in the case of PDLLA-Si ($n = 20$) the theoretical SiO_2 content was 3.4%. In both cases the calculated values satisfactorily agree with the experimental results. Hence, TGA results confirm the reliability of NMR analysis.

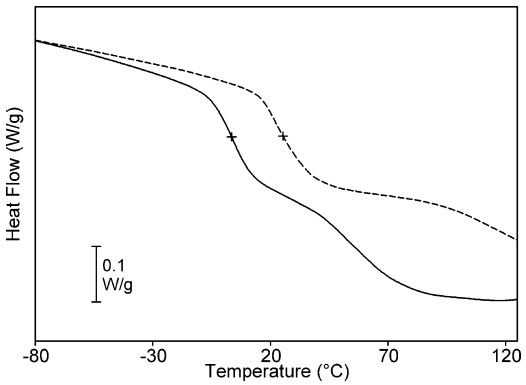

Figure 2. DSC curves of the first (solid line) and second (dashed line) heating scans of A25-0. The glass transition temperature is marked by a plus sign on the curves.

Synthesis and Characterization of the Hybrids. A preliminary attempt to obtain hybrids from direct solubilization of the functionalized polymeric precursors (PDLLA-Si) in the liquid TEOS reactant in the presence of H_2O and HCl was not successful. Hence, THF was used as the solvent, and the synthesis of ceramers was carried out at room temperature.[20] Shrinking and cracking problems, associated with weight loss during the sol−gel process and thus more significant with a high TEOS content, were overcome by lowering the evaporation rate of volatile byproducts as described in the Experimental Section.

None of the synthesized hybrids, after rt gelation (i.e., A*X*-0 and B*X*-0), were thermally stable above rt. As an example, Figure 2 shows two subsequent DSC scans of A25-0 up to 130 °C; after the first heating run, in the second scan the glass transition temperature (T_g) undergoes a 30 °C upshift that highlights a decrease of the polymer chain mobility. The first scan also displays a broad endotherm starting around 40 °C, attributed to vaporization in the DSC pan of sol−gel byproducts, as earlier suggested by Tian et al. for similar systems.[20] The present results indicate that additional sol−gel reactions are promoted as the temperature increases slightly above rt, leading to sample weight loss (5.6% after the two heating scans shown in Figure 2) and to a T_g increase. A remarkable weight loss in the temperature range from rt to 200 °C is also observed by TGA, as reported in Table 1. All hybrids obtained by the sol−gel process at rt (without further thermal treatment) show significant weight losses from rt to 200 °C. No T_g values are reported for such thermally unstable ceramers.

Thermal curing treatments were performed to force the reaction to yield thermally stable ceramers in the temperature range of their potential use (rt to 120 °C). The effect of vacuum application associated with heating was also investigated. The TGA results, collected in Table 1, show that the weight loss from rt to 200 °C is very much reduced after the hybrids are cured at 130 °C, being absent in both A25-130 and A50-130 and in the range of 1.5% in all other ceramers. Hybrids cured at 80 °C under vacuum display intermediate weight losses.

The differently cured samples were subjected to DSC measurements with the aim of studying the influence of the thermal history on the hybrid properties. The effect of two different heat treatments on the same sample composition is shown in Figure 3, where the DSC curves of A25 after thermal curing at 80 °C under vacuum and after curing at 130 °C (namely, hybrids A25-80V and A25-130) are reported. The only observed transition in both samples is a glass transition, whose temperature depends on the applied thermal treatment (Table 2). No endothermal features attributable to further curing appear

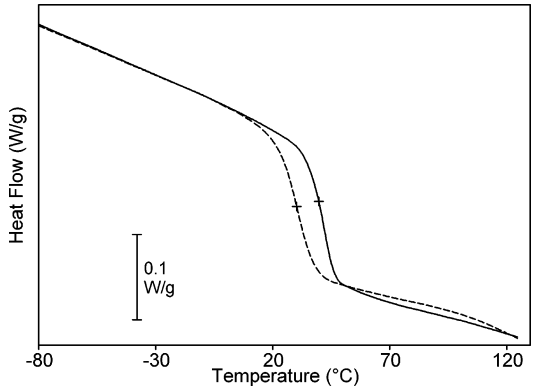

Figure 3. DSC curves (first scan) of A25-80V (dashed line) and A25-130 (solid line). The glass transition temperature is marked by a plus sign on the curves.

Table 2. Thermal Properties of A Series and B Series Hybrids

A series			B series	
sample	T_g[a] (°C)	T_α[b] (°C)	sample	T_g[a] (°C)
A25-80V	30	43	B25-80V	14
A25-130	39	47	B25-130	32
A50-80V	34	50	B50-80V	26
A50-130	47	57	B50-130	40
A75-80V	*c*	nd	B75-80V	*c*
A75-130	*c*	nd	B75-130	*c*

[a] By DSC, first heating scan. [b] By DMTA. [c] Not defined due to the presence of a broad endotherm overlapping the glass transition.

above rt. Both hybrids display reproducible DSC curves in subsequent DSC scans up to 130 °C (not shown), demonstrating that thermally stable situations, characterized by different T_g values, are obtained by the two curing treatments applied (80V and 130). The absence of additional cross-linking reactions during the DSC runs of Figure 3 is not surprising for the ceramer cured at 130 °C, because the DSC scan does not exceed the curing temperature. In the case of the hybrid cured at 80 °C the observed behavior may be explained by the action of the vacuum applied during the heat treatment, which helps remove sol−gel byproducts. Consequently, early vitrification locks the polymer chains in a 3-D network. As for the difference in T_g values of the two A25 hybrids of Figure 3, it is suggested that different hydrolysis/condensation equilibria set in during the sol−gel process carried out in different conditions. As a result, the network formed in the ceramer cured at 80 °C under vacuum is less motionally restricted (lower T_g) than that of the hybrid cured at higher temperature without a vacuum. The DSC results suggest that A25-80V is unable to undergo additional curing during the heating run from 80 to 130 °C. Hence, the weight loss observed for this hybrid by TGA (3.4% between rt and 200 °C) is likely to occur between 130 and 200 °C.

What is reported in Figure 3 for A25 is also observed for A50, with T_g values shifted to higher temperatures, consistent with the higher inorganic phase content of A50 hybrids (Table 2). Conversely, a different behavior is observed for the A75 ceramer that does not reach a thermally stable situation after either of the heat treatments reported above (80V and 130). Moreover, while in the thermograms of both thermally treated A50 and thermally treated A25 no transition is present below 130 °C other than T_g (see Figure 3), in both A75-80V and A75-130 a broad endothermal peak appears above rt in the DSC scans (not shown). This behavior is attributed to the release of volatile byproducts of the sol−gel process that is incomplete

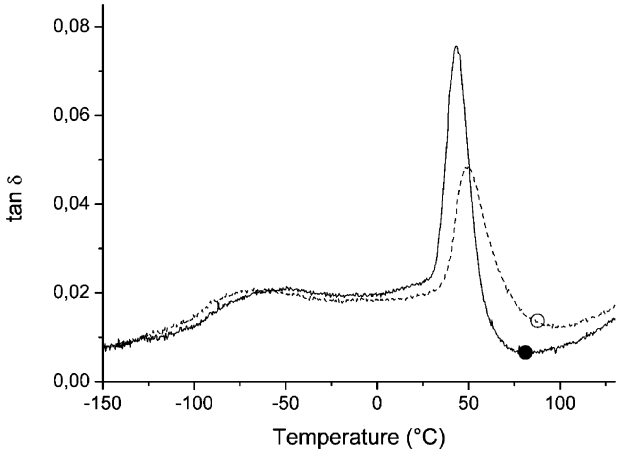

Figure 4. DMTA curves of A25-80V (solid line, ●) and A50-80V (dashed line, ○).

after the applied curing conditions and continues during the DSC scan in the high TEOS content A75 ceramers. Due to the presence of the mentioned broad endothermal peak, it is not possible to evaluate T_g for the A75 hybrids.

The thermally cured A series ceramers investigated by DSC were also analyzed by DMTA after the hybrid films were sandwiched between two aluminum plates to provide the convenient support for the measurement of the viscoelastic spectrum in bending mode,[49] and the results are reported in Table 2. In Figure 4 the loss factor curves of two hybrids with different inorganic phase contents and the same curing treatment (A25-80V and A50-80V) are presented. Both DMTA spectra show a main relaxation process (α) associated with the glass transition and a low-temperature secondary dissipation region (β). The α relaxation broadens, shifts to higher temperature, and is reduced in intensity when the TEOS content in the sol−gel feed increases (i.e., going from A25 to A50). This behavior reflects the change in the ceramer composition as well as the expected loss of organic phase mobility. The DMTA curves of the corresponding series A hybrids cured at 130 °C (A25-130 and A50-130, curves not shown) display an analogous trend with changing inorganic phase content, although in this case the α peaks are centered at higher temperatures, in good agreement with the trend observed in the calorimetric T_g values (compare T_α and T_g in Table 2). No DMTA measurements were run on hybrids with 75% TEOS in the feed.

Series B ceramers show similar trends of T_g with changing thermal treatment and composition as discussed above for series A hybrids (Table 2). It is interesting to compare the thermal behavior of ceramers of the two series (A and B) with the same content of TEOS in the feed and same curing treatment. Figure 5 displays this comparison for ceramers containing 50% TEOS in the feed. After each of the curing procedures applied, the hybrid synthesized from the shorter precursor (A50-130 and A50-80V, curves a and c) exhibits a higher glass transition temperature than that of the corresponding ceramer containing the longer PDLLA oligomer (B50-130 and B50-80V, respectively, curves b and d). This behavior reflects the stronger motional hindrance that bound silica particles exert on shorter polymer chains. Analogous trends are shown by the glass transition of the ceramers containing 25% TEOS in the feed (Table 2).

All hybrids prepared in this work, independent of the thermal curing applied, were optically transparent as shown in Figure 6 for A50-130. Transparency of organic−inorganic hybrids is usually taken as an indication of phase domains with submi-

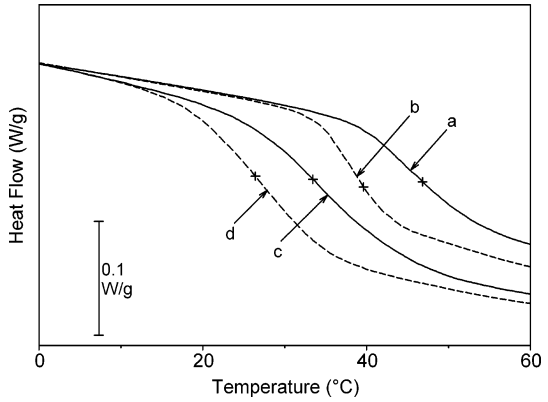

Figure 5. DSC curves (first scan) of A50-130 (curve a), B50-130 (curve b), A50-80V (curve c), and B50-80V (curve d).

Figure 6. Transparent A50-130 film (0.25 mm thick). The hybrid sample shape is outlined by the black line for the sake of easy location.

crometric (nanometric) dimensions. A preliminary AFM analysis of this specimen (Figure 7), performed in tapping mode and in phase-imaging mode, highlights the intimate nanometric structure of the hybrid material. While the topographic study shows that the film surface is globally very flat (with an rms roughness of 0.37 nm), as evident in Figure 7A, the phase image shows the presence of homogeneously dispersed hard particles (clear objects in Figure 7B). The observed hard objects, interpreted as silica particles, have an average apparent area of 175 nm^2. AFM evidence of hard domains dispersed in a matrix with different viscoelastic behavior has been previously reported for ceramers.[55,56] The present results show that optical transparency of the analyzed hybrid originates from its nanostructure.

Radiopacity of the A series ceramers was tested using standard mammographic equipment. Figure 8 shows the radiographic image of two samples of A75-130 in film form (thickness 0.26 mm). The shape of both samples is clearly discernible as a bright (radiopaque) area contrasting with the dark (radiotransparent) background. In the case of hybrids with lower silica content (pictures not shown) the ceramer radiographic picture is still very visible, although the contrast becomes weaker with decreasing silica fraction. Radiopacity of the present PLA-based hybrids is therefore demonstrated.

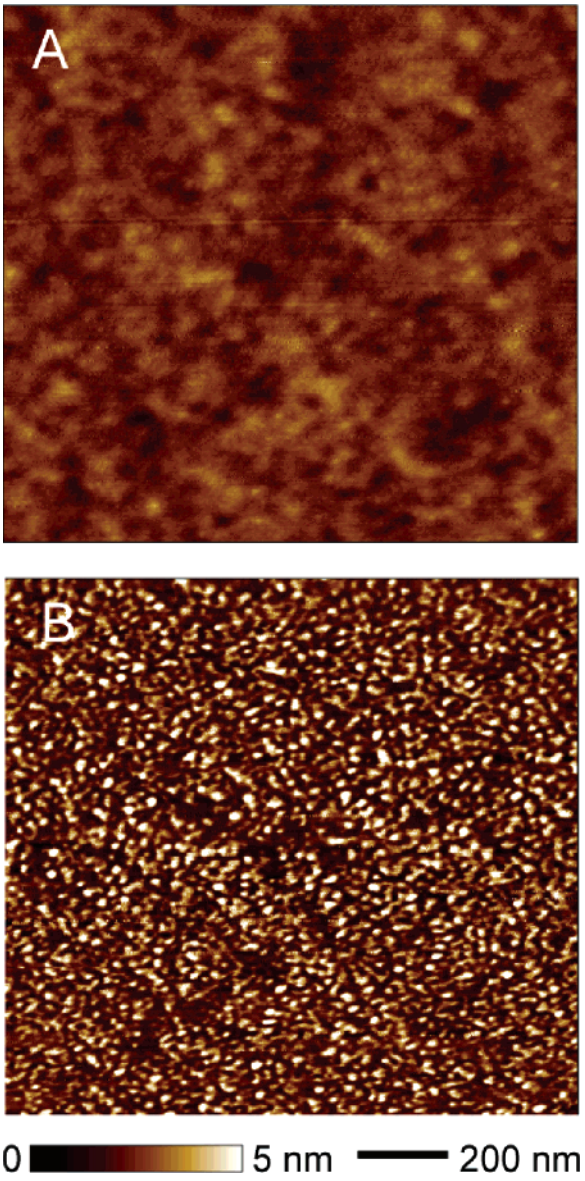

Figure 7. Tapping-mode AFM topography (A) and phase-contrast image (B) of a specimen of A50-130. The height of features in the topographic image are coded according to the attached color map. The phase contrast is coded in shades on the same color map, so that lighter areas represent harder regions of the specimen (interpreted as silica particles).

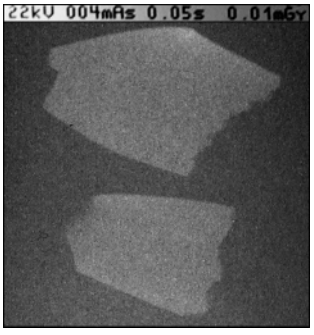

Figure 8. Radiographic image of A75-130 films.

Further studies are under way with the aim to assess the suitability of such ceramers to be applied as thin coatings to different substrates, taking into account coating thickness, silica content, and PLA oligomer chain length.

CDV

Conclusions

The synthesis and characterization of PDLLA-Si was carried out by an easy two-step procedure, without addition of catalysts and with the minimum use of solvent. Good control over the average molecular weight of the two PDLLA-OH oligomers synthesized ($n = 10, 20$) was achieved, and they were both used as organic phase precursors in the sol−gel synthesis of hybrids with TEOS. The thermal and viscoelastic properties of the cured hybrids show that different heat treatments (thermal curing at 80 °C under vacuum and curing at 130 °C without a vacuum) on the same sample composition lead to different glass transition temperatures, owing to different sol−gel process kinetics. In addition, hybrids obtained from the shorter PLA precursor, investigated by DSC and DMTA show a higher glass transition temperature than the corresponding ceramer containing the longer PLA oligomer.

All hybrids are transparent and radiopaque. This latter feature may have interesting implications in the application of these materials as coatings for biomedical devices requiring radiographic localization.

Acknowledgment. We gratefully thank Prof. Stefano Mignani and Mrs. Rita Luciani (Centro Mammografico, Policlinico Universitario Sant'Orsola, Bologna University) for the radiographic measurements. Financial support by MIUR (PRIN 2004, Prot. 2004030304) is gratefully acknowledged.

References and Notes

(1) Yano, S.; Iwata, K.; Kurita, K. *Mater. Sci. Eng., C* **1998**, *6*, 75−81.
(2) Ochi, M.; Takahashi, R.; Tenanchi, A. *Polymer* **2001**, *42*, 5151−5158.
(3) Wilkes, G. L.; Orler, B.; Huang, H. *Polym. Prepr. (Am. Chem. Soc., Div. Polym. Chem.)* **1985**, *26*, 300−301.
(4) Schmidt, H. *J. Non-Cryst. Solids* **1985**, *73*, 681−691.
(5) Okada, A.; Usuki, A. *Mater. Sci. Eng.* **1995**, *C3*, 109−115.
(6) Gilman, J. W.; Jackson, C. L.; Morgan, A. B.; Harris Jr., R.; Manias, E.; Giannelis, E. P.; Wuthenow, M.; Hilton, D.; Phillips, S. H. *Chem. Mater.* **2000**, *12*, 1866−1873.
(7) Porter, D.; Metcalfe, E.; Thomas, M. J. K. *Fire Mater.* **2000**, *24*, 45−52.
(8) Zanetti, M.; Lomakin, S.; Camino, G. *Macromol. Mater. Eng.* **2000**, *279*, 1−9.
(9) Armes, S. P. *Polym. News* **1995**, *20*, 233−237.
(10) Godovski, D. Y. *Adv. Polym. Sci.* **1995**, *119*, 79−122.
(11) Caseri, W. *Macromol. Rapid Commun.* **2000**, *21*, 705−722.
(12) Kickelbick, G. *Prog. Polym. Sci.* **2003**, *28*, 83−114.
(13) Huang, H. H.; Orler, B.; Wilkes, G. L. *Macromolecules* **1987**, *20*, 1322−1330.
(14) Kohjiya, S.; Ochiai, K.; Yamashita, S. *J. Non-Cryst. Solids* **1990**, *119*, 132−135.
(15) Surivet, F.; Lam, T. M.; Pascault, J. P.; Nai, C. *Macromolecules* **1992**, *25*, 5742−5751.
(16) Huang, H. H.; Glaser, R. H.; Wilkes, G. L. *ACS Symp. Inorg. Org. Polym.* **1987**, *360*, 354.
(17) Huang, H. H.; Wilkes, G. L. *Polym. Bull.* **1987**, *18*, 455−462.
(18) Brennan, A. B.; Wang, B.; Rodrigues, D. E.; Wilkes, G. L. *J. Inorg. Org. Polym.* **1991**, *1*, 167−187.
(19) Brennan, A. B.; Wilkes, G. L. *Polymer* **1991**, *32*, 733−739.
(20) Tian, D.; Dubois, P.; Jerome, R. *J. Polym. Sci., Part A: Polym. Chem.* **1997**, *35*, 2295−2305.
(21) Tian, D.; Dubois, P.; Jerome, R. *Polymer* **1996**, *37*, 3983−3987.
(22) Tian, D.; Blancher, S.; Dubois, P.; Jerome, R. *Polymer* **1998**, *39*, 855−864.
(23) Saegusa, T. *J. Macromol. Sci., Pure Appl. Chem.* **1991**, *A28*, 817−829.
(24) Noell, J. L. W.; Wilkes, G. L.; Mohanty, D. K.; McGrath, J. E. *J. Appl. Polym. Sci.* **1990**, *40*, 1177−1194.
(25) Messori, M.; Toselli, M.; Pilati, F.; Fabbri, E.; Fabbri, P.; Pasquali, L.; Nannarone, S. *Polymer* **2004**, *45*, 805−813.
(26) Wen, J.; Wilkes, G. L. *Chem. Mater.* **1996**, *8*, 1667−1681.
(27) Kokubo, T.; Kim, H.-M.; Kawashita, M. *Biomaterials* **2003**, *24*, 2161−2175.
(28) Dong, S.; Chen, X. *Rev. Mol. Biotechnol.* **2002**, *82*, 303−323.
(29) Vert, M.; Schwarch, G.; Coudane, J. *J. Macromol. Sci., Pure Appl. Chem.* **1995**, *A32*, 787−796.
(30) Kohn, J.; Abramson S. In *Biomaterials science: an introduction to materials in medicine*, 2nd ed.; Ratner, B. D., Hoffman, A. S., Schoen, F. J., Lemons, J. E., Eds.; Elsevier Academic Press: Amsterdam, 2004; Chapter 2.
(31) Ikada, Y.; Tsuji, H. *Macromol. Rapid Commun.* **2000**, *21*, 117−132.
(32) Albertsson, A. C.; Varma, I. K. *Biomacromolecules* **2003**, *4*, 1466−1486.
(33) Torchilin, V. P. *Adv. Drug Delivery Rev.* **2002**, *54*, 235−252.
(34) Kohn, J.; Zeltinger, J. *Expert Rev. Med. Devices* **2005**, *2*, 667−671.
(35) Jayakrishnan, A.; Thanoo, B. C. *Biomaterials* **1990**, *11*, 477−481.
(36) Thanoo, B. C.; Sunny, M. C.; Jayakrishnan, A. *Biomaterials* **1991**, *12*, 525−528.
(37) Thanoo, B. C.; Sunny, M. C.; Jayakrishnan, A. *J. Appl. Biomater.* **1991**, *2*, 67−72.
(38) Cabasso, I.; Smid, J.; Sahni, S. K. *J. Appl. Polym. Sci.* **1989**, *38*, 1653−1666.
(39) Cabasso, I.; Smid, J.; Sahni, S. K. *J. Appl. Polym. Sci.* **1990**, *41*, 3025−3042.
(40) Moszner, N.; Saiz, U.; Klester, A. M.; Rheinberger, V. *Angew. Makromol. Chem.* **1995**, *224*, 115−123.
(41) Horak, D.; Metalova, M.; Svec, F.; Drobnik, J.; Katal J.; Borovicka, M.; Adamyan, A. A.; Voronkova, O. S.; Gumargalieva, K. Z. *Biomaterials* **1987**, *8*, 142−145.
(42) Jayakrishnan, A.; Thanoo, B. C.; Rathinam, K.; Mohanty, M. *J. Biomed. Mater. Res.* **1990**, *24*, 993−1004.
(43) Mottu, F.; Rufenacht, D. A.; Laurent, A.; Doelker, E. *Biomaterials* **2002**, *23*, 121−131.
(44) Nirmala, R. J.; Juby, P.; Jayakrishnan, A. *Biomaterials* **2006**, *27*, 160−166.
(45) Dobson, P. J. U.S. Patent 5876783, 1999; *Chem. Abstr.* **1999**, *130*, 213672.
(46) Sahagian, R. U.S. Patent 7077837, 2006.
(47) Glocker, D. A.; Romach, M. M. U.S. Patent Application, US 2005288773 A1, 2005; *Chem. Abstr.* **2005**, *144*, 74958.
(48) Bearinger, C. R.; Camilletti, R. C.; Haluska, L. A.; Michael, K. W. U.S. Patent 5399441, 1995; *Chem. Abstr.* **1995**, *122*, 328491.
(49) Ceccorulli, G.; Zini, E.; Scandola, M. *Macromol. Chem. Phys.* **2006**, *207*, 864−869.
(50) Jedlinski, Z.; Walach, W.; Kurcok, P.; Adamus, G. *Macromol. Chem. Phys.* **1991**, *192*, 2051−2057.
(51) Jedlinski, Z.; Kurcok, P.; Lenz, R. W. *J. Macromol. Sci., Pure Appl. Chem.* **1995**, *A32*, 797−810.
(52) Helminen, A.; Korhonen, H.; Seppala, J. V. *Polymer* **2001**, *42*, 3345−3353.
(53) Jamshidi, K.; Hyon, S. H.; Ikada, Y. *Polymer* **1988**, *29*, 2229−2234.
(54) Ho, K. L. G.; Pometto, A. L.; Hinz, P. N. *J. Environ. Polym. Degrad.* **1999**, *7*, 83−92.
(55) Tian, T.; Dubois, P.; Grandfils, C.; Jerome, R.; Viville, P.; Lazzaroni, R.; Bredas, J. L.; Leprince, P. *Chem. Mater.* **1997**, *9*, 871−874.
(56) Amerio, E.; Sangermano, M.; Malucelli, G.; Priola, A.; Voit, B. *Polymer* **2005**, *46*, 11241−11246.

BM060921N